

BioProAgent: Neuro-Symbolic Grounding for Constrained Scientific Planning

Yuyang Liu¹, Jingya Wang¹, Liuzhenghao Lv¹, Yonghong Tian^{1,†}

¹School of Electronic and Computer Engineering, Peking University

{liyuyang13, yhtian}@pku.edu.cn, {lvliuzh}@stu.pku.edu.cn

Abstract

Large language models (LLMs) have demonstrated significant reasoning capabilities in scientific discovery but struggle to bridge the gap to physical execution in wet-labs. In these irreversible environments, probabilistic hallucinations are not merely incorrect, but also cause equipment damage or experimental failure. To address this, we propose **BioProAgent**, a neuro-symbolic framework that anchors probabilistic planning in a deterministic Finite State Machine (FSM). We introduce a State-Augmented Planning mechanism that enforces a rigorous *Design-Verify-Rectify* workflow, ensuring hardware compliance before execution. Furthermore, we address the context bottleneck inherent in complex device schemas by *Semantic Symbol Grounding*, reducing token consumption by $\sim 6\times$ through symbolic abstraction. In the extended BioProBench benchmark, BioProAgent achieves 95.6% physical compliance (compared to 21.0% for ReAct), demonstrating that neuro-symbolic constraints are essential for reliable autonomy in irreversible physical environments.¹

1 Introduction

Large Language Models (LLMs) are increasingly shifting from static knowledge retrieval to active world modeling in scientific discovery. In the Self-Driving Laboratories (SDL) (Stein and Gregoire, 2019; Abolhasani and Kumacheva, 2023), LLMs serve as central cognitive engines. Specifically, categorized as Agentic AI (Sapkota et al., 2025; Gridach et al., 2025), they design complex chemical synthesis schemes (Boiko et al., 2023), discover novel materials (Ghafarollahi and McCarthy, 2024), and laboratory assistants (Darvish et al., 2025). Recently, multi-agent systems (Jin et al., 2025; Zhou

¹Code at <https://github.com/YuyangSunshine/bioproagent> and project at <https://yuyangsunshine.github.io/BioPro-Project/>

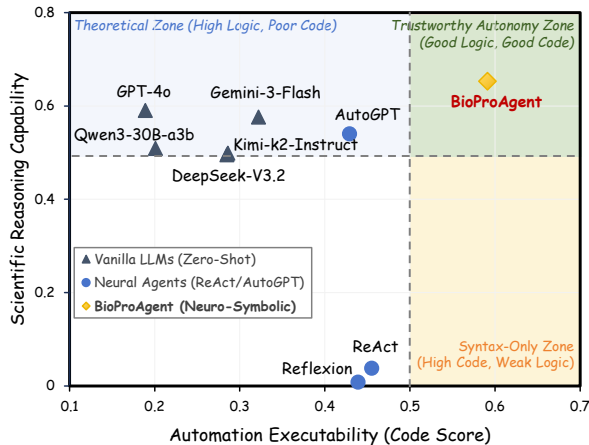


Figure 1: *Scientific Reasoning vs. Automation Executability*. **Vanilla LLMs** occupy the *Theoretical Zone* (high logic, weak code), while **Neural Agents** (like **ReAct**) often generating better code but failing in scientific reasoning. **BioProAgent** achieves *Trustworthy Autonomy* with superior performance in both dimensions.

et al., 2025) have demonstrated impressive capabilities in biological reasoning and computational workflow orchestration. However, a critical **Execution Gap** (Wang and et al., 2024) emerges when transitioning from computer simulation predictions to in vitro physical experiments. Despite the remarkable physical autonomy achieved by robotic platforms, from mobile robotic chemists (Burger et al., 2020) to autonomous materials synthesis labs (Szymanski et al., 2023), they still operate under rigid, task-specific workflows. Unlike reversible code and virtual environments in software engineering, due to irreversible physical laws, any deviation in parameters can lead to catastrophic equipment failures, sample loss, or unreproducible experimental results in biological experimental environments.

Despite the reasoning capabilities of existing scientific agents, they still face key challenges in high-risk automated applications. First, standard agents (Yao et al., 2022; Shinn et al., 2023) suffer from Cognitive Drift, where contextual overload leads

to process confusion, resulting in skipped critical steps or confused temporal dependencies. While current memory systems (Chhikara et al., 2025; Packer et al., 2023) excel at semantic retrieval, they struggle with lossless tracking of distinct physical entities. A slight “lost-in-the-middle” (Liu et al., 2024) confusion between similar reagent IDs can cause experimental failure. More critically, there is a distinct lack of Pre-Execution Interlocks. While previous neuro-symbolic methods like PAL (Gao et al., 2023), Program-of-Thoughts (Chen et al., 2022), and SayCan (Ahn et al., 2022) have combined LLMs with planners to improve logical correctness, they primarily focus on reasoning optimality. They cannot handle the strict and irreversible safety constraints in wet labs because they lack deterministic control mechanisms based on physical rules that stop and self-correct before execution.

To address these challenges, we propose a neuro-symbolic **BioProAgent** for achieving trustworthy autonomy (Figure 1), which grounds probabilistic reasoning in a deterministic backbone network with a training-free **Finite State Machine (FSM)**. Unlike static agents restricted to pre-defined workflows, BioProAgent flexibly adapts to diverse tasks by using FSM as a safety boundary to enforce a rigorous “Design-Verify-Rectify” workflow. This controller ensures that all hardware instructions must undergo hierarchical verification for both scientific logic and physical safety before being issued. Furthermore, to address context challenges, we introduce **Semantic Symbol Grounding**. By decoupling the high-dimensional payloads into symbolic pointers, we reduce token consumption by $\sim 6\times$ while ensuring 100% resource consistency. Extensive evaluation on extended BioProBench (Liu et al., 2025b) shows that BioProAgent achieves an 88.7% success rate in error recovery, compared to a complete failure (0%) for the standard baseline.

Our contributions are summarized as follows:

- We propose BioProAgent, a training-free neuro-symbolic framework that bridges the gap between probabilistic reasoning and deterministic physical execution.
- We introduce a State-Augmented Planning mechanism driven by a deterministic FSM and a Semantic Symbol Grounding technique that effectively addresses context problem.
- Extensive experiments demonstrate BioProAgent achieves state-of-the-art performance in

scientific validity and physical consistency, and significantly outperforms baselines.

2 Related Works

2.1 LLM Agents for Scientific Discovery

Autonomous research has evolved from basic tool usage (Bran et al., 2023; Boiko et al., 2023) to complex multi-agent collaboration (Zhang et al., 2025; Jin et al., 2025; Huang et al., 2025). Recent frameworks like DeepScientist (Weng et al., 2025) and Organa (Darvish et al., 2025) demonstrate long-horizon autonomy, and BioMARS (Qiu et al., 2025) and AutoLabs (Panapitiya et al., 2025) introduce domain-specific visual monitoring and self-correction. AI-native operating systems (Sim et al., 2024; Fei et al., 2024; Gao et al., 2025) are also continuously strengthening the execution infrastructure. However, despite these advances, a critical gap remains: a lack of cognitive safety interlocking mechanisms, making general-purpose agents vulnerable to irreversible physical damage.

2.2 Neuro-Symbolic Reasoning & Action

Coupling LLMs with symbolic planners or code interpreters, such as PAL (Gao et al., 2023), Program-of-Thoughts (Chen et al., 2022), and LLM+P (Liu et al., 2023), significantly boosts logical and planning accuracy. In embodied settings, SayCan (Ahn et al., 2022) and Voyager (Wang et al., 2023) ground actions in physical affordances, while iterative frameworks like ReAct (Yao et al., 2022) and Reflexion (Shinn et al., 2023) improve reasoning via verbal feedback. While these methods are effective in completing tasks in reversible or simulated environments, they lack mechanisms for enforcing irreversible safety constraints.

2.3 Long-Horizon Context Management

While Longformer (Beltagy et al., 2020) and RAG (Lewis et al., 2020) extend context windows, they often fragment the coherent narrative essential for protocol execution. Agent-specific memory systems like MemGPT (Packer et al., 2023) and Mem0 (Chhikara et al., 2025) maintain multi-session coherence through hierarchical compression. Recent approaches such as ACON (Kang et al., 2025) and LLM-State (Chen et al., 2023) address long-horizon tasks via learned state compression. However, these purely neural methods remain probabilistic and inherently lossy, making them vulnera-

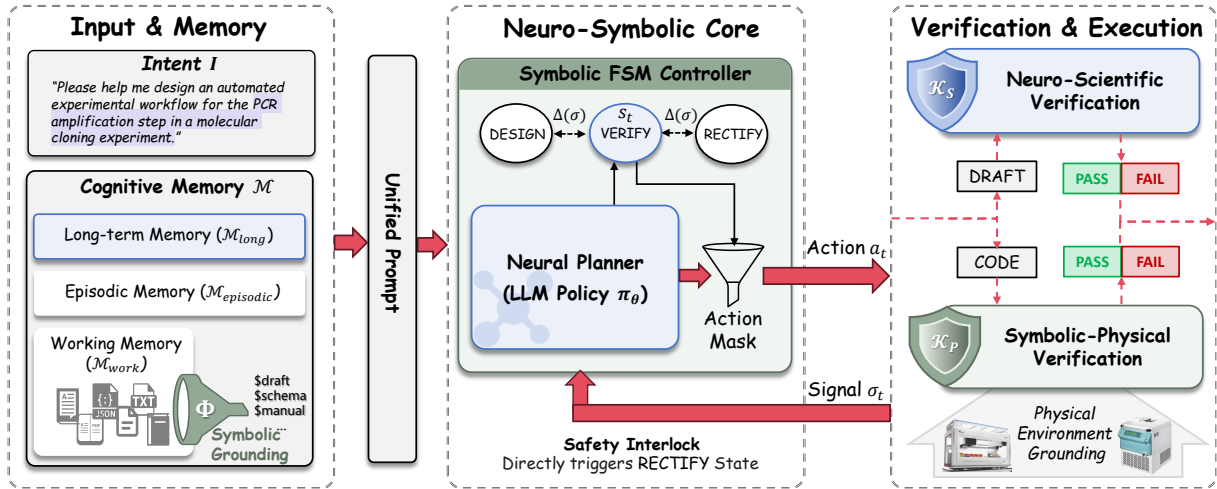


Figure 2: **Overview of BioProAgent.** (1) Cognitive Memory utilizes Symbolic Grounding Φ to manage context efficiently; (2) Neural Planner π_θ is grounded in a Design-Verify-Rectify FSM $\Delta(\sigma)$; (3) Hierarchical Verification ($\mathcal{K}_s, \mathcal{K}_p$) acts as a safety interlock, enforcing physical compliance by deterministically triggering rectification.

ble to “lost-in-the-middle” phenomenon (Liu et al., 2024). This ambiguity is unacceptable for tracking precise scientific entities like reagent IDs.

3 Methodology

We formulate automated biological protocol generation as a constrained scientific planning problem. Let \mathcal{P} denote possible protocol sequences derived from the valid action space \mathcal{A} defined by the Hardware Registry Ω . Given an intent I and an environmental context \mathcal{E} , our goal is to identify the optimal executable protocol $P^* \in \mathcal{P}$ that is scientifically valid and physically executable, as:

$$P^* = \operatorname{argmax}_{P \in \mathcal{P}} \mathbb{P}_\theta(P|I) \cdot \mathbb{I}[\mathcal{K}_s(P)] \cdot \mathbb{I}[\mathcal{K}_p(P)], \quad (1)$$

where $\mathbb{I}[\cdot]$ is indicator function. \mathcal{K}_s and \mathcal{K}_p are the Scientific and Physical verification functions, respectively. (Summary of notations in Appendix A.)

3.1 Hybrid Cognitive Memory Architecture

Existing agents often suffer from cognitive drift in long-horizon tasks, where early context regarding reagent IDs is lost. To address this, we design a hierarchical memory system $\mathcal{M} = \langle \mathcal{M}_{work}, \mathcal{M}_{episodic}, \mathcal{M}_{long} \rangle$, which decouples reasoning logic from high-dimensional data payloads.

Structured Working Memory \mathcal{M}_{work} . Direct input of raw JSON schemas (often >10k tokens) induces context saturation. We propose **Semantic Symbol Grounding**, projecting artifacts into

symbol-value pairs $\{(k, v)\}$. During planning, context is compressed via a projection function Φ :

$$C_{context} \leftarrow \Phi(\mathcal{M}_{work}) = \{k_i \mid (k_i, v_i) \in \mathcal{M}_{work}\}. \quad (2)$$

For execution, a generated symbolic action a_t is grounded via a resolution function Ψ : $a_t^{exec} \leftarrow \Psi(a_t, \mathcal{M}_{work})$, which maps pointers k back to physical parameters v . This reduces processing complexity from $\mathcal{O}(|v|)$ to $\mathcal{O}(j)$ where $j \ll |v|$, ensuring the planner focuses on logic flow rather than data processing.

Episodic and Long-term Memory. We use episodic Memory $\mathcal{M}_{episodic}$ to track the active trajectory $\tau_t = [(a_0, o_0), \dots]$ and long-term Memory \mathcal{M}_{long} to retrieve knowledge, ensuring global consistency across different experimental sessions.

The prompt concatenates retrieved knowledge, episodic history, and grounded symbols to form a unified context for reasoning.

3.2 State-Augmented Neuro-Symbolic Plan

To address the lack of strict adherence to state-related rules required by safety-critical hardware in probabilistic LLMs, BioProAgent uses a deterministic finite state machine (FSM) to decouple reasoning from control, aiming to enforce a rigorous Design-Verify-Rectify (DVR) workflow. Formally defined as $FSM = \langle \mathcal{S}, \Sigma, \mathcal{A}, \Delta, \pi_\theta \rangle$, unlike finite state automata used in traditional robots which hard-code specific operation sequences (e.g., Move_A_to_B), our states (e.g., DESIGN, VERIFY, RECTIFY) control the cognitive processes of generation and verification, as illustrated in Fig. 2.

Algorithm 1 BioProAgent FSM-Gated Execution

Require: User Intent I , Hardwares Ω , Knowledge \mathcal{M}_{long}

Ensure: Protocol P^* or Failure

```
1: Initialize:  $\mathcal{M}_{work} \leftarrow \text{Parse}(I)$ ,  $s_0 \leftarrow \text{INIT}$ 
2: Initialize: Trajectory  $\tau \leftarrow []$ , Signal  $\sigma \leftarrow \mathbf{0}$ 
3: while  $s_t \neq \text{SUCCESS}$  and  $t < T_{max}$  do
4:    $s_t \leftarrow \Delta(\sigma)$  {Refer to Priority Matrix (Tab. 1)}
5:   if  $s_t \in \{\text{RECTIFY\_DRAFT or \_CODE}\}$  then
6:     Update prompt via  $\sigma$ 
7:   end if
8:   Generate  $a_t \sim \pi_\theta(a|s_t, \Phi(\mathcal{M}_{work}), \tau)$ 
9:   if  $a_t$  is Draft then
10:    Check:  $\mathcal{K}_s(a_t)$ ; Update:  $\sigma_{sci}$ 
11:   else if  $a_t$  is Code then
12:    Check:  $\mathcal{K}_p(a_t, \Omega)$ ; Update:  $\sigma_{phys}$ 
13:    if  $\neg\sigma_{phys}$  then
14:       $\sigma \leftarrow \text{INTERLOCK}\{\text{ForceTransition}\}$ 
15:    else
16:      Append to  $P^*$ ;  $\tau \leftarrow \tau \cup \{a_t\}$ 
17:    end if
18:   end if
19:   Update Memory  $\mathcal{M}_{episodic}$  with  $(s_t, a_t, \sigma)$ 
20: end while
21: return  $P^*$ 
```

This abstraction allows BioProAgent to maintain a consistent control architecture across different domains, from molecular cloning to chemical synthesis, without requiring architectural reconstruction.

3.2.1 Neuro-Symbolic Control Engine

Define $\Sigma = \{0, 1\}^5$ as the space of context signals. Let $\sigma_t \in \Sigma$ be the signal at time t . State transitions $\Delta : \mathcal{S} \times \Sigma \rightarrow \mathcal{S}$ are governed by a deterministic *Priority Decision Matrix* (Table 1). The physical execution function E_{phys} for an action a_t is defined as:

$$E_{phys}(a_t) = \begin{cases} \text{Execute}(a_t), & \text{if } s_t = \text{APPROVED} \wedge \sigma_{phys}^+ \\ \emptyset, & \text{otherwise (Interlock Triggered)} \end{cases} \quad (3)$$

We formalize the system’s reliability as a conditional safety guarantee: $P(\text{Unsafe} \mid \text{Interlock}, \mathcal{K}_\Omega, \Phi) \approx 0$. Interlock denotes the FSM gating mechanism. The guarantee holds under two assumptions: (1) \mathcal{K}_Ω : the hardware registry Ω completely covers the physical constraints; and (2) Φ : the semantic symbol grounding correctly maps natural language intents to specific device IDs.

For unmodeled risks outside Ω , the system defaults to a HALT state to ensure safety. The FSM evaluates the ordering rules and selects the target state based on the highest-priority signal match:

$$s_{t+1} = \Delta(\sigma_t, s_t) = \text{Target}(r_j) \in s_{t+1} \in \mathcal{S} \quad (4)$$

where $j = \min\{i \mid \text{Match}(r_i, \sigma_t)\}$. As shown in Table 1, if technical validation fails, the interlock strictly prohibits execution. The complete

Table 1: **FSM Priority Decision Matrix.** See Appendix C for the complete definition.

Signal Condition (σ_t)	Priority	Target State (s_{t+1})
$\sigma_{phys}^- \wedge \sigma_{code}$	1	RECTIFY_CODE
$\sigma_{sci}^- \wedge \sigma_{draft}$	2	RECTIFY_DRAFT
$\neg\sigma_{draft} \wedge \sigma_{know}$	3	DESIGN_DRAFT
$\sigma_{draft} \wedge \sigma_{sci}^+$	4	DESIGN_CODE
$\sigma_{draft} \wedge \neg\sigma_{sci}$	5	VERIFY_DRAFT
$\sigma_{code} \wedge \sigma_{phys}^+$	6	SUCCESS
...

neuro-symbolic execution, coordinating the interaction between $\Delta(\sigma)$ and π_θ , is formalized in Algorithm 1.

3.2.2 Neural Reasoning Policy

In each state s_t , π_θ selects an action a_t from \mathcal{A} corresponds to the set of available tools (Appendix B), which is categorized into three functional clusters: (1) **Design** (Generation), (2) **Verify** (Validation), and (3) **Rectify** (Correction). To ensure coherence, the FSM dynamically prunes the action space to $\mathcal{A}_{valid} \subset \mathcal{A}$ based on the active phase in s_t . The planner is conditioned on s_t , and the system prompt explicitly enforces this state-dependent action masking (Appendix H.1).

3.3 Hierarchical Verification Framework

To implement the **Verify** phase of the DVR loop, we employ a two-layer hierarchical framework to enforce the constraints in Eq. (1).

Layer 1: Neuro-Scientific Verification (\mathcal{K}_s).

The Scientific Reflector assesses the **Design** draft using prompts derived from expert-in-the-loop iterations. This ensures the CoT reasoning (Wei et al., 2022) follows professional wet-lab standards rather than superficial syntax checking.

$$\mathbb{I}[\mathcal{K}_s(P_{draft})] \iff \text{Reflector}(P, \text{Task}) \rightarrow \text{“PASS”}. \quad (5)$$

Full verification criteria, including controls and biosafety checks, are detailed in Appendix H.2.

Layer 2: Symbolic-Physical Verification (\mathcal{K}_p).

To ensure safety, a deterministic *Rule Engine* (\mathcal{R}_{phys}) verifies the generated Code against the hardware registry Ω . Ω encodes constraints for 22 instruments across Liquid Handling (LH), Thermal Control (TC), and Centrifugation (CF). Crucially, any violation ($\neg K_p$) triggers the **Rectify** interlock:

$$\mathbb{I}[\mathcal{K}_p(P_{code})] = \prod_{op \in P} \prod_{c \in \Omega(\text{device}_{op})} \mathbb{I}[\text{Check}(op, c)]. \quad (6)$$

Table 2: **The BioProAgent Evaluation Framework.** Metrics are categorized by dimension, improvement direction (\uparrow/\downarrow), and evaluation source.

Dimension	Evaluator	Key Metrics
Scientific	Semantic Match	S_{sem} (\uparrow), ROUGE-L (\uparrow)
	LLM-as-a-Judge	C_s (\uparrow)
Physical	Rule Engine	S_{code} (\uparrow), C_p (\uparrow)
	Ground Truth	Acc_{seq} (\uparrow), Acc_{param} (\uparrow)
Efficiency	System Logs	$Succ.$ (\uparrow), Tokens (\downarrow), Loop Rate (\downarrow)

4 Experiments

4.1 Experimental Setup

Benchmark and Hardware Grounding. We evaluate our framework using an extended version of BioProBench (Liu et al., 2025b), including four specialized subsets: **Subset A (Protocol Drafting)** assesses scientific validity; **Subset B (Code Generation)** evaluates hardware schema compliance and parameter accuracy; **Subset C (Long-Horizon)** targets global orchestration, featuring 9 complex protocols with 547 atomic steps (max 238 per task); and **Subset D (Error Correction)** measures robustness against injected faults. To ensure reproducibility, the complete source code, the digitized hardware registry (Ω) covering 22 core synthetic biology instruments, and the dataset are provided in the supplementary material. Crucially, although evaluated in simulation, all generated instructions strictly adhere to the API specifications of standard automated devices to bridge the sim-to-real gap.

Baselines. We compare BioProAgent against three categories of baselines: (1) **Vanilla LLMs:** GPT-4o (Islam and Moushi, 2025), Gemini-3-Flash (Google, 2025), DeepSeek-V3.2 (Liu et al., 2025a), and Kimi-k2-instruct (Team et al., 2025) via direct prompting; (2) **Standard Agents:** ReAct (Yao et al., 2022), Reflexion (Shinn et al., 2023), and AutoGPT (Yang et al., 2023); (3) **Domain-Specific Agent:** Biomni (Huang et al., 2025) (evaluated on native protocol generation). *Critical Implementation Detail:* To ensure fair comparison, all standard agent baselines were equipped with the exact same toolset as BioProAgent.

Evaluation Framework We evaluate performance across three dimensions: (1) **Scientific Validity:** Measured by a composite *Semantic Score* S_{sem} for keyword coverage and an LLM-as-a-Judge *Scientific Score* C_s for procedural logic. (2) **Physical Compliance:** Quantified by the *Overall Code*

Score S_{code} , which aggregates *Physical Compliance* C_p verified by the symbolic rule engine, along with *Sequence Accuracy* Acc_{seq} and *Parameter Accuracy* Acc_{param} . Notably, S_{code} acts as a hard gatekeeper: schema format failures yield a zero score. (3) **System Efficiency:** Tracks *Success Rate* $Succ.$, token consumption *Tokens*, and *Loop Rate*. Table 2 summarizes these metrics; mathematical derivations are detailed in Appendix D.

4.2 Main Results

4.2.1 Scientific Reasoning (Subset A).

As shown in Table 3, BioProAgent achieves a Scientific Validity Score (C_s) of 0.591, a **30% improvement** over the strongest agent baseline (ReAct) and almost double that of vanilla models (Gemini-3-Flash). Notably, even the domain-specialized Biomni only reaches a C_s of 0.342, highlighting that domain knowledge alone is insufficient without structured reasoning constraints. Paired t-tests confirm that these improvements are statistically significant ($p < 0.001$). BioProAgent’s advantage stems from its *Scientific Reflector* within the FSM, which requires a formal review of scientific logic before proceeding to the coding phase, whereas standard agents often neglect crucial controls in pursuit of rapid generation. Cross-model validation (Pearson $r \geq 0.84$) confirms the robustness of our LLM-as-a-Judge metric (see Appendix D.4.2).

4.2.2 Physical Compliance (Subset B).

Table 3 reveals significant differences in code generation performance between the baselines. Vanilla LLMs maintain $C_p = 0.995$ primarily by defaulting to conservative, low-complexity code, which naturally results in poor Parameter Accuracy (0.295). Standard Agents (e.g., ReAct), conversely, attempt complex operations but suffer from catastrophic safety failures ($C_p = 0.210$). *Although ReAct was equipped with the exact same Rule Engine tool, it often fails to invoke these tools proactively due to context saturation or a lack of stopping conditions.* BioProAgent effectively eliminates this trade-off, achieving the highest S_{code} and ACC_{param} while maintaining high-quality security ($C_p = 0.956$). This confirms FSM’s deterministic gating is essential for enforcing safety checks that probabilistic agents tend to bypass.

Table 3: Main Results on Protocol Drafting (Subset A) and Code Generation (Subset B). †: indicates statistical significance compared to all baselines (Biomni, ReAct, AutoGPT, Reflexion) with $p < 0.001$ (paired t-test).

Method	Backbone	Subset A: Scientific Reasoning				Subset B: Hardware Execution		
		ROUGE-L \uparrow	S_{sem} \uparrow	C_s † \uparrow	Time (s) \downarrow	S_{code} \uparrow	C_p \uparrow	Acc_{param} \uparrow
Direct	GPT-4o	0.107	0.202	0.189	13.8	0.590	0.995	0.295
Direct	Gemini-3-Flash	0.130	0.247	0.322	12.1	0.576	0.996	0.287
Direct	DeepSeek-V3	0.123	0.260	0.285	52.1	0.495	0.995	0.205
Biomni	(Specialized)	0.081	0.252	0.342	87.1	N/A	N/A	N/A
ReAct	Gemini-3-Flash	0.116	0.268	0.455	44.5	0.038	0.210	0.103
Reflexion	Gemini-3-Flash	0.118	0.282	0.439	148.4	0.278	0.534	0.403
AutoGPT	Gemini-3-Flash	0.116	0.258	0.429	119.6	0.540	0.911	0.468
BioProAgent	Gemini-3-Flash	0.147	0.344	0.591	71.8	0.653	0.956	0.610

Table 4: Main Results on Long-Horizon Stability (Subset C) and Error Correction (Subset D). Bold indicates the best performance within agent-based frameworks.

Method	Backbone	Subset C: Long-Horizon Stability			Subset D: Error Correction		
		Succ. \uparrow	Acc_{param} \uparrow	C_p \uparrow	ACC_{seq} \uparrow	C_p \uparrow	Loop Rate \downarrow
ReAct	Gemini-3-Flash	88.9%	0.114	0.217	0.0%	0.000	40.0%
Reflexion	Gemini-3-Flash	33.3%	0.000	0.000	0.0%	0.000	0.0%
AutoGPT	Gemini-3-Flash	66.7%	0.409	0.644	0.0%	0.000	0.0%
BioProAgent	Gemini-3-Flash	100.0%	0.718	0.950	0.464	0.887	0.0%

4.2.3 Long-Horizon Stability (Subset C).

As shown in Table 4, standard agents exhibit significant performance gaps when the workflow expands to an average of 60 steps. While AutoGPT maintains a 66.7% success rate, its lack of a structural stopping condition leads to inefficient thought loops and excessive token consumption. ReAct achieves an 88.9% task completion rate, but its low physical consistency ($C_p = 0.217$) and $Acc_{param} = 0.114$ reveal ID drift. *Notably, Reflexion fails completely in $Acc_{param} = 0.000$. This is attributed to “Schema Corruption”: its verbal feedback mechanism frequently injects conversational artifacts (e.g., apologies) into the JSON payload, causing the strict rule engine to fail to parse the output.* In contrast, by replacing the high-dimensional data payloads with symbolic pointers, our *Semantic Symbol Grounding* ensures 100% resource consistency and lossless state tracking.

4.2.4 Error Correction (Subset D).

Subset D evaluates the system’s ability to diagnose and correct injected physical violations, as shown in Table 4. All baseline agents exhibit a 0% correction rate, with ReAct entering infinite retry loops in 40% of scenarios. This shows that without a deterministic controller, probabilistic LLMs naturally prioritize sequence plausibility over physical safety. BioProAgent restores physical safety (C_p)

to 0.887, significantly outperforming the baselines (0.0). The neuro-symbolic FSM acts as a deterministic router: when a violation is detected by the rules engine, it overwrites the LLM’s trajectory and forces a transition to the RECTIFY_CODE state. This allows the agent to align its outputs with hardware limitations, demonstrating a robust self-correcting capability essential for trustworthy automated science. Appendix E.2 provides a detailed analysis of logical errors, resource errors, and physical errors.

4.3 Holistic Capability Assessment

Fig. 3a visualizes the capability envelope of each agent. Crucially, this chart aggregates performance across diverse benchmarks: while C_p and S_{code} appear on multiple axes, they correspond to distinct stress tests, standard generation (Subset B), long-horizon stability (Subset C), and error correction (Subset D). Existing methods exhibit significant capability biases: Direct Prompting (Grey) defaults to conservative safety (C_p) but fails in complex coordination, while ReAct (Green) improves scientific reasoning (C_s) at the cost of severe physical hallucinations. BioProAgent effectively eliminates this trade-off, achieving a balanced pentagonal coverage. The performance gap is most significant in Long-Horizon and Self-Correction dimensions. While baselines degrade to near-zero performance due to context collapse or open-loop error propa-

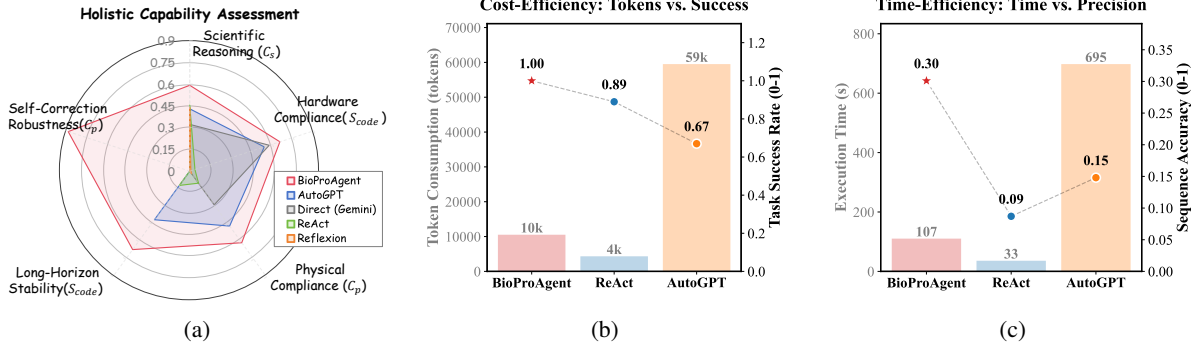


Figure 3: **Efficiency and Reliability Analysis.** (a) **Multidimensional Capabilities:** BioProAgent (red) achieves the most expansive capability envelope across five critical dimensions. Note that identical metrics on different axes represent performance in distinct evaluation subsets. (b) **Cost-Efficiency:** On long-horizon tasks (Subset C), our system reduces token consumption by 82% compared to AutoGPT while maintaining a 100% success rate. (c) **Time-Efficiency:** BioProAgent demonstrates superior precision with concise execution time.

gation, BioProAgent maintains robustness, demonstrating that neuro-symbolic FSM is essential for sustaining trustworthy autonomy in high-stakes environments.

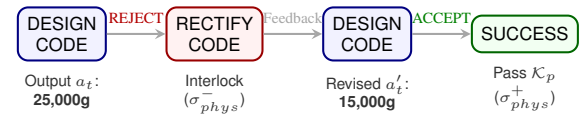
4.4 Efficiency and Cost Analysis

As shown in Fig. 3(b), BioProAgent consumes **82% fewer tokens** than the AutoGPT on Subset C. This efficiency stems from our *Semantic Symbol Grounding* mechanism, which maintains a near-constant context size by substituting dense data payloads with symbolic pointers, thereby mitigating the “context explosion” inherent in the recursive summarization. Furthermore, Fig. 3(c) highlights the critical trade-off between execution time and precision. While standard baselines are faster, they lack the requisite precision for complex hardware operations. While the AutoGPT attains moderate precision, its execution time is prohibitively long (avg. 695s). BioProAgent achieves an optimal balance, delivering high-precision results with competitive execution speeds and the widest safety margin (C_p), validating practical viability for the real-world laboratory deployment.

4.5 Qualitative Analysis

Mechanism of Correction. Standard LLM agents typically operate in an open-loop manner: when a dangerous parameter for an hallucinate is generated, execution is immediate, inevitably leading to failure. In contrast, Fig. 4 illustrates the FSM’s correction mechanism in action, effectively intercepting speed limit violations. In the physical violation case (Fig. 4a), the *Symbolic Rule Engine* (\mathcal{K}_p) preemptively intercepts this violation ($V > V_{max}$), triggering a forced state transition

(a) Physical Violation ($V > V_{max}$)



(b) Symbol Grounding Error (Undefined ID)

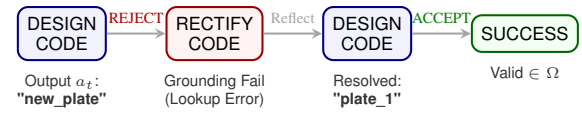


Figure 4: **FSM-Driven Self-Correction Trajectories.** (a) Physical Correction. (b) Symbol Grounding Repair.

Table 5: **Representative Error Corrections in Subset D.** The FSM interceptor enforces the **Rectify** phase, guiding the agent from violations to valid execution.

Constraint	Design Violation (s_{design})	FSM Rectification ($s_{rectify}$)
Physical (\mathcal{K}_p)	centrifuge(speed='25000g') × Exceeds rotor limit (15k)	centrifuge(speed='15000g') ✓ Clamped to safety max
Symbol (Φ)	transfer(source='buffer_x') × Grounding Fail (No ID)	transfer(source='trough_1') ✓ Remapped to registry
Causal	seal_plate(); transfer(...) × Blocked op (Sealed)	transfer(...); seal_plate() ✓ Reordered dependency

to RECTIFY_CODE. This forces the Neural Planner to recognize the specific error signal (σ_{phys}^-) and regenerate the code within safe limits (15,000g). Similarly, for a logical hallucination case (Fig. 4b), the system detects semantic drift (an undefined resource ID new_plate”). The FSM prevents this error propagation, guiding the agent to remap the action to the grounded symbol plate_1”.

Granularity of Rectification. Table 5 further demonstrates that these corrections are not merely stochastic retries but involve semantic-level reasoning. We observe three distinct categories of recti-

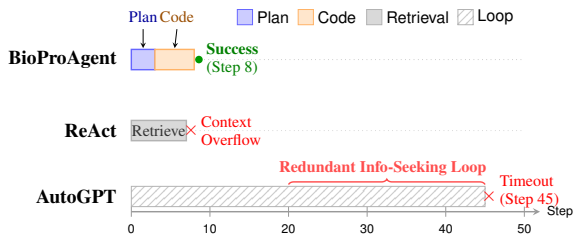


Figure 5: **Trace Analysis (Subset C)**. Execution divergence on a long-horizon task. TOP: BioProAgent efficiently transitions to coding via FSM. MIDDLE: ReAct fails early due to context overflow. BOTTOM: AutoGPT wastes resources in a retrieval loop.

fication within the DVR loop: (1) **Safety Alignment**: Adjusting physical parameters to satisfy hardware constraints (\mathcal{K}_p); (2) **Resource Grounding**: Resolving hallucinated variables to physically validated slots via the projection function Φ ; and (3) **Causal Rectification**: Correcting logical dependencies, such as the critical reordering of `seal_plate()` operations. This confirms that BioProAgent’s neuro-symbolic core effectively operationalizes a “Design-Verify-Rectify” workflow, ensuring trustworthy execution in high-stakes environments.

Log-Level Behavioral Analysis. To diagnose why baseline agents fail in long-horizon tasks despite having access to the same tools, we visualize the execution trajectories of a representative metabolomics workflow in Fig. 5. ReAct terminates prematurely (Step 7) as retrieved API schemas saturate its context window, blocking valid action generation. Lacking a deterministic *stop* signal, AutoGPT enters an infinite loop of redundant `retrieve_knowledge` calls (Steps 20–45), consuming excessive tokens without advancing state. In contrast, BioProAgent’s FSM enforces a rigid *Plan* \rightarrow *Code* transition, acting as a cognitive clock that ensures efficient completion in just 8 steps.

4.6 Ablation Study

Table 6 quantitatively validates the architectural necessity of each component. **Impact of FSM**: Removing the FSM controller leads to a structural failure. The Scientific Validity (C_s) degrades to 0.262, while performance on long-horizon (Subset C) and error-correction (Subset D) tasks collapses to near-zero (0.000). This confirms that deterministic state transitions are not merely auxiliary, but foundational for sustaining the planning-execution loop and triggering self-healing mechanisms. **Impact of**

Table 6: Ablation Study of BioProAgent Components.

Variant	Subset A	Subset B	Subset C	Subset D
	C_s	C_p	S_{code}	C_p
Full Model	0.591	0.956	0.668	0.887
w/o FSM	0.262	0.049	0.000	0.000
w/o Verification	0.563	0.902	0.648	0.870
w/o Knowledge	0.561	0.889	0.657	N/A
w/o Clarify	0.403	N/A	0.632	N/A

Verification: Ablating the verifications ($\mathcal{K}_p, \mathcal{K}_s$) causes C_p to drop from 0.956 to 0.902. While less dramatic than the FSM ablation, this deficit demonstrates that neural inference alone, even with advanced prompting, cannot guarantee the zero-defect safety required for irreversible wet-lab automation. **Impact of Knowledge & Clarification**: Omitting the *Clarify* tool or external knowledge significantly impairs reasoning. Notably, the sharp decline in C_s ($0.591 \rightarrow 0.403$) without clarification underscores the critical role of human-in-the-loop disambiguation for handling under-specified protocols. Statistical significance is further confirmed via cross-judge verification (Appendix D.4.1) and paired t-tests (Appendix D.4.2).

5 Conclusion

We present BioProAgent, a neuro-symbolic framework addressing the critical execution gap in autonomous scientific discovery. By grounding probabilistic LLM reasoning within a deterministic Finite State Machine, BioProAgent enforces a “Design-Verify-Rectify” workflow for irreversible wet-lab environments. Evaluations on extended BioProBench demonstrate that BioProAgent achieves SOTA performance and demonstrates robust autonomous self-correction where traditional agents fail. Our work emphasizes that, for high-risk physical applications, neural intelligence must be constrained by symbolic safety interlocks to ensure trustworthy and reliable autonomy.

Limitations & Future Work

Despite its performance, BioProAgent has some limitations. First, the framework’s security relies on a predefined hardware registry (Ω). While effective for known instruments, this requires manual registration for custom hardware. Future work will explore using a multimodal logic model (LLM) to automate this process by directly reading the device manual. Additionally, our current evaluation was conducted in high-fidelity simulations using

standard APIs. While this validates the correctness of the logic and parameters, real-world physical randomness remains unmodeled. Integrating a real-time visual feedback loop is crucial for managing these physical variables.

References

- Milad Abolhasani and Eugenia Kumacheva. 2023. The rise of self-driving labs in chemical and materials sciences. *Nature Synthesis*, 2(6):483–492.
- Michael Ahn, Anthony Brohan, Noah Brown, Yevgen Chebotar, Omar Cortes, Byron David, Chelsea Finn, Chuyuan Fu, Keerthana Gopalakrishnan, Karol Hausman, and 1 others. 2022. Do as i can, not as i say: Grounding language in robotic affordances. *arXiv preprint arXiv:2204.01691*.
- Iz Beltagy, Matthew E Peters, and Arman Cohan. 2020. Longformer: The long-document transformer. *arXiv preprint arXiv:2004.05150*.
- Daniil A Boiko, Robert MacKnight, Ben Kline, and Gabe Gomes. 2023. Autonomous chemical research with large language models. *Nature*, 624(7992):570–578.
- Andres M Bran, Sam Cox, Andrew D White, and Philippe Schwaller. 2023. Chemcrow: Augmenting large-language models with chemistry tools. *arXiv preprint arXiv:2304.05376*.
- Benjamin Burger, Phillip M Maffettone, Vladimir V Gusev, Catherine M Aitchison, Yang Bai, Xiaoyan Wang, Xiaobo Li, Ben M Alston, Buyi Li, Rob Clowes, and 1 others. 2020. A mobile robotic chemist. *Nature*, 583(7815):237–241.
- Siwei Chen, Anxing Xiao, and David Hsu. 2023. Llm-state: Open world state representation for long-horizon task planning with large language model. *arXiv preprint arXiv:2311.17406*.
- Wenhu Chen, Xueguang Ma, Xinyi Wang, and William W Cohen. 2022. Program of thoughts prompting: Disentangling computation from reasoning for numerical reasoning tasks. *arXiv preprint arXiv:2211.12588*.
- Prateek Chhikara, Dev Khant, Saket Aryan, Taranjeet Singh, and Deshraj Yadav. 2025. Mem0: Building production-ready ai agents with scalable long-term memory. *arXiv preprint arXiv:2504.19413*.
- Kourosh Darvish, Marta Skreta, Yuchi Zhao, Naruki Yoshikawa, Sagnik Som, Miroslav Bogdanovic, Yang Cao, Han Hao, Haoping Xu, Alán Aspuru-Guzik, Animesh Garg, and Florian Shkurti. 2025. *Or-gana: A robotic assistant for automated chemistry experimentation and characterization*. Preprint, arXiv:2401.06949.
- Yuxing Fei, Bernardus Rendy, Rishi Kumar, Olympia Dartsi, Hrushikesh P Sahasrabudhe, Matthew J McDermott, Zheren Wang, Nathan J Szymanski, Lauren N Walters, David Milsted, and 1 others. 2024. Alabos: a python-based reconfigurable workflow management framework for autonomous laboratories. *Digital Discovery*, 3(11):2275–2288.
- Jing Gao, Junhan Chang, Haohui Que, Yanfei Xiong, Shixiang Zhang, Xianwei Qi, Zhen Liu, Jun-Jie Wang, Qianjun Ding, Xinyu Li, and 1 others. 2025. Unilabos: An ai-native operating system for autonomous laboratories. *arXiv preprint arXiv:2512.21766*.
- Luyu Gao, Aman Madaan, Shuyan Zhou, Uri Alon, Pengfei Liu, Yiming Yang, Jamie Callan, and Graham Neubig. 2023. Pal: Program-aided language models. In *International Conference on Machine Learning*, pages 10764–10799. PMLR.
- Alireza Ghafarollahi and Markus J McCarthy. 2024. Sciagents: Automating scientific discovery through bioinspired multi-agent collaborative language modeling. *Advanced Materials*.
- Google. 2025. Gemini 3 flash: A capable and insightful ai thought partner. <https://gemini.google.com/>. Accessed: 2025-12-29.
- Mourad Gridach, Jay Nanavati, Khaldoun Zine El Abidine, Lenon Mendes, and Christina Mack. 2025. Agentic ai for scientific discovery: A survey of progress, challenges, and future directions. *arXiv preprint arXiv:2503.08979*.
- Kexin Huang, Serena Zhang, Hanchen Wang, Yuanhao Qu, and 1 others. 2025. *Biomni: A general-purpose biomedical ai agent*. Preprint.
- Raisa Islam and Owana Marzia Moushi. 2025. Gpt-4o: The cutting-edge advancement in multimodal llm. In *Intelligent Computing-Proceedings of the Computing Conference*, pages 47–60. Springer.
- Ruofan Jin, Yucheng Guo, Yuanhao Qu, Ming Yang, and 1 others. 2025. *Biolab: End-to-end autonomous life sciences research with multi-agents system integrating biological foundation models*. Preprint.
- Minki Kang, Wei-Ning Chen, Dongge Han, Huseyin A Inan, Lukas Wutschitz, Yanzhi Chen, Robert Sim, and Saravan Rajmohan. 2025. Acon: Optimizing context compression for long-horizon llm agents. *arXiv preprint arXiv:2510.00615*.
- Patrick Lewis, Ethan Perez, Aleksandra Piktus, Fabio Petroni, Vladimir Karpukhin, Naman Goyal, Heinrich Küttler, Mike Lewis, Wen-tau Yih, Tim Rocktäschel, and 1 others. 2020. Retrieval-augmented generation for knowledge-intensive nlp tasks. *Advances in neural information processing systems*, 33:9459–9474.

- Aixin Liu, Aoxue Mei, Bangcai Lin, Bing Xue, Bingxuan Wang, Bingzheng Xu, Bochao Wu, Bowei Zhang, Chaofan Lin, Chen Dong, and 1 others. 2025a. Deepseek-v3. 2: Pushing the frontier of open large language models. *arXiv preprint arXiv:2512.02556*.
- Bo Liu, Yuqian Jiang, Xiaohan Zhang, Qiang Liu, Shuo Zhang, Joydeep Biswas, and Peter Stone. 2023. Llm+p: Empowering large language models with optimal planning proficiency. *arXiv preprint arXiv:2304.11477*.
- Nelson F Liu, Kevin Lin, John Hewitt, Ashwin Paranjape, Michele Bevilacqua, Fabio Petroni, and Percy Liang. 2024. Lost in the middle: How language models use long contexts. *Transactions of the Association for Computational Linguistics*, 12:157–173.
- Yuyang Liu, Liuzhenghao Lv, Xiancheng Zhang, Li Yuan, and Yonghong Tian. 2025b. Bioprobench: Comprehensive dataset and benchmark in biological protocol understanding and reasoning. *arXiv preprint arXiv:2505.07889*.
- Charles Packer, Vivian Fang, Shishir G Patil, Kevin Lin, Sarah Wooders, and Joseph E Gonzalez. 2023. Memgpt: Towards llms as operating systems.
- Gihan Panapitiya, Emily Saldanha, Heather Job, and Olivia Hess. 2025. Autolabs: Cognitive multi-agent systems with self-correction for autonomous chemical experimentation. *arXiv preprint arXiv:2509.25651*.
- Yibo Qiu, Zan Huang, Zhiyu Wang, Handi Liu, Yiling Qiao, Yifeng Hu, Shu'ang Sun, Hangke Peng, Ronald X Xu, and Mingzhai Sun. 2025. Biomars: A multi-agent robotic system for autonomous biological experiments. *arXiv preprint arXiv:2507.01485*.
- Ranjan Sapkota, Konstantinos I Roumeliotis, and Manoj Karkee. 2025. Ai agents vs. agentic ai: A conceptual taxonomy, applications and challenges. *arXiv preprint arXiv:2505.10468*.
- Noah Shinn, Federico Cassano, Ashwin Gopinath, Karthik Narasimhan, and Shunyu Yao. 2023. Reflexion: Language agents with verbal reinforcement learning. *Advances in Neural Information Processing Systems*, 36:8634–8652.
- Malcolm Sim, Mohammad Ghazi Vakili, Felix Strieth-Kalthoff, Han Hao, Riley J Hickman, Santiago Miret, Sergio Pablo-García, and Alán Aspuru-Guzik. 2024. Chemos 2.0: An orchestration architecture for chemical self-driving laboratories. *Matter*, 7(9):2959–2977.
- Helge S Stein and John M Gregoire. 2019. Progress and prospects for accelerating materials science with automated and autonomous workflows. *Chemical science*, 10(42):9640–9649.
- Nathan J Szymanski, Bernardus Rendy, Yuxing Fei, Rishi E Kumar, Tanjin He, David Milsted, Matthew J McDermott, Max Gallant, Ekin Dogus Cubuk, Amil Merchant, and 1 others. 2023. An autonomous laboratory for the accelerated synthesis of novel materials. *Nature*, 624(7990):86–91.
- Kimi Team, Yifan Bai, Yiping Bao, Guanduo Chen, Jiahao Chen, Ningxin Chen, Ruijue Chen, Yanru Chen, Yuankun Chen, Yutian Chen, and 1 others. 2025. Kimi k2: Open agentic intelligence. *arXiv preprint arXiv:2507.20534*.
- Guanzhi Wang, Yuqi Xie, Yunfan Jiang, Ajay Mandlekar, Chaowei Xiao, Yuke Zhu, Linxi Fan, and Anima Anandkumar. 2023. Voyager: An open-ended embodied agent with large language models. *arXiv preprint arXiv:2305.16291*.
- Xiaoxuan Wang and et al. 2024. Scibench: Evaluating college-level scientific problem-solving abilities of large language models. *arXiv preprint arXiv:2307.10635*.
- Jason Wei, Xuezhi Wang, Dale Schuurmans, Maarten Bosma, Fei Xia, Ed Chi, Quoc V Le, Denny Zhou, and 1 others. 2022. Chain-of-thought prompting elicits reasoning in large language models. *Advances in neural information processing systems*, 35:24824–24837.
- Yixuan Weng, Minjun Zhu, Qiuqie Xie, Qiyao Sun, Zhen Lin, Sifan Liu, and Yue Zhang. 2025. Deepscientist: Advancing frontier-pushing scientific findings progressively. *arXiv preprint arXiv:2509.26603*.
- Hui Yang, Sifu Yue, and Yunzhong He. 2023. Auto-gpt for online decision making: Benchmarks and additional opinions. *arXiv preprint arXiv:2306.02224*.
- Shunyu Yao, Jeffrey Zhao, Dian Yu, Nan Du, Izhak Shafran, Karthik R Narasimhan, and Yuan Cao. 2022. React: Synergizing reasoning and acting in language models. In *The eleventh international conference on learning representations*.
- Zhen Zhang, Zhichu Ren, Chia-Wei Hsu, Weibin Chen, Zhang-Wei Hong, Chi-Feng Lee, Aubrey Penn, Hongbin Xu, Daniel J Zheng, Shuhan Miao, and 1 others. 2025. A multimodal robotic platform for multi-element electrocatalyst discovery. *Nature*, pages 1–3.
- Yuyang Zhou, Jin Su, Jiawei Zhang, Wangyang Hu, Tianli Tao, Guanqi Li, Xibin Zhou, Li Fan, and Fajie Yuan. 2025. Prime: A multi-agent environment for orchestrating dynamic computational workflows in protein engineering. *bioRxiv*, pages 2025–09.